 CMES, vol.3, no.3, pp.399-415, 2002

A Green's Function for Variable Density Elastodynamics under Plane Strain Conditions by Hormander's Method

George D. Manolis [1], **Stavros Pavlou** [2]

Abstract: A free-space Green's function for problems involving time-harmonic elastic waves in variable density materials under plane strain conditions is developed herein by means of Hormander's method in the context of matrix algebra formalism. The challenge when solving problems involving inhomogenous media is that the coefficients appearing in the governing equations of motion are position-dependent. Furthermore, an additional difficulty stems from the fact that these governing equations are vectorial, which implies that coordinate transformation techniques that have been successful with scalar waves can no longer be used. Thus, the present work aims at establishing the necessary background that will allow for construction of Green's functions for a general class of inhomogeneous media that is not necessarily restricted to the variable density case. These functions, besides being useful in their own right, are also important within the context of boundary integral formulations, where they appear as kernels in the underlying integral equations. Finally, a numerical example serves to illustrate the proposed methodology and to quantify the influence of a variable density profile on the propagation of elastic waves.

keywords: Boundary integrals; Elastodynamics; Green's function; Hormander's method; Inhomogeneous media; Wave equation.

1 Introduction

The development of Green's functions for elastic wave propagation in solids is of engineering importance, because these functions represent fundamental solutions to special types of disturbances (such as the point force and the unit dislocation) and under rather broad boundary conditions (such as the Sommerfeld radiation). At the same time, they comprise an essential part (namely the kernels) of any boundary integral equation method (BIEM) formulation (Cruse and Rizzo 1968; Cruse 1968) and, of course, of its corresponding numerical solution technique, the boundary element method (BEM) (Manolis and Beskos 1988; Dominguez 1993). The latter method has been very successful in solving boundary-value problems of engineering importance in transient elastodynamics, as can be deduced by consulting the extensive literature reviews by Beskos (1987; 1997) that span the last fifteen years. Since the preferred formulation is invariably a displacement-traction approach based on Somigliana's identity, the corresponding Green's functions must come from a solution of the equations of elastodynamics for a point force and under radiation-type boundary conditions. This can be done by a variety of ways, e.g., use of potentials (Helmholtz potentials, Stokes potentials), displacement vector decomposition into dilatational and rotational components (Miklowitz, 1978), use of the dynamic equivalent to Galerkin's vector, integral transforms (Duffy, 1994), etc.

The major difficulty has been an extension of the aforementioned methodologies to problems involving other categories of materials, which go beyond the homogeneous, isotropic linear elastic continuum, such as those exhibiting heterogeneity, anisotropy, layering, randomness, etc. (Ewing et al., 1957, Hanyga, 1985). Applications, however, are numerous and span various engineering fields, including seismic prospecting, earthquake engineering, acoustics, ocean engineering, signal transmission, composite materials and non-destructive testing evaluation to name a few. The most complicated structure to model is, of course, the earth itself (Helbig, 1994).

A recent, and rather extensive, literature review on wave motion in non-homogeneous materials can be found in Manolis and Shaw (2000). In order to add to this list of efforts regarding solution of boundary-value problems with the purpose of recovering Green's functions for various types of inhomogeneities, we mention the work of Selvadurai and Lan (1998) on a half-space under axisym-

[1] Aristotle University of Thessaloniki, Greece
[2] University of Patras, Greece

metric conditions with elastic parameters that are periodic functions of the depth, of Vardoulakis and Georgiadis (1997) on the use of gradient elasticity theory in modeling the microstructure of a half-space under *SH* waves, of Muravskii and Operstein (1996) on time harmonic vibrations of an incompressible half-space whose shear modulus exhibits a linear variation with depth, and of Hryniewicz and Filipkowski (1996) on the construction of dynamic stiffness matrices for in-plane motion in a material with a shear modulus that is a random function of the depth. Furthermore, Guzina and Pak (1996) computed Green's functions for point and ring loads sources in a half-space with a smoothly varying material profile, while Vrettos (1998) examined the case of a vertical point load on the surface of a half-space with a non-zero shear modulus at its surface that varies with depth but remains bounded at infinite depth. The method of solution in all the above works is integral transforms, with preference given to the Hankel transform. The exception to this is Hryniewicz and Filipkowski (1996), whose problem has to do with random vibrations and therefore requires a different technique, namely one that hinges on the solution of a system of first-order differential equations. Recently, Melnikov and Melnikov (2001) introduced the concept of modified potentials, which are used for computing Green's functions for biharmonic equations defined in 2D regions with complex configurations. It is thus possible to model materials consisting of arbitrary shaped regions with different material properties. Finally, Gragg (1998) used an energy conservation approach to examine Helmholtz's equation for a weakly non-uniform material, i.e., a material with a slowly varying density profile. The interesting thing about this last case is the possibility of forward-moving 1*D* wave motion only, with very little backscattering.

As previously mentioned, the aforementioned Green's functions, besides being useful in their own right, are also used as kernels in BEM formulations for the purpose of solving complex problems numerically. Specifically, recent work on BEM formulations is that of Ang et al. (1996) and of Clements (1998) for the general second order, elliptic partial differential operator with non-constant coefficients that are functions of two spatial variables, of Xu and Kamiya (1998) on the inhomogeneous Poisson equation whose linear part is governed by Laplace' operator and of Itagaki (2000), who used the dual reciprocity BEM to handle Helmholtz's equation with a spatially-dependent source term.

As far as applications are concerned, we have the construction of compliance matrices for a rigid punch in the elastic half-plane, whose coefficients are exponentially decaying functions of two spatial coordinates (Bakirtas, 1984), the use of a 1*D* inhomogeneous shear beam to model the earthquake response of hill-shaped landfills (Gunturi and Elgamal, 1998), the computation of synthetic seismograms for both laterally and vertically heterogeneous geological deposits (Geller and Ohminate, 1994), the evaluation of dispersion curves for wave motion guided through anisotropic beams with variable cross-section geometry (Volovoi et al., 1998) and the computation of eigenvalues for continuously nonhomogeneous membranes of variable density (Wang, 1998). Also, Hazanov (1999) used Huet's method for determining the effective material properties of heterogeneous elastic materials with imperfect interfaces, while Muravskii (2000) used earlier solutions to interpret experimental results for waves propagating across the surface of a half-space so as to deduce the degree of inhomogeneity in its material properties, i.e., an inverse-type of problem.

Finding other, simpler methods of solution to problems involving continuous media with non-constant material parameters is difficult. In this respect, we briefly mention some recent activity in the area of time harmonic acoustic waves in heterogeneous media using a coordinate transformation method based on conformal mapping (Shaw and Manolis, 2000a). While this approach is limited to 2*D* problems and is "inverse" in its form, i.e., a given mapping will lead to a particular type of heterogeneity, it represents a step forward in the development of fundamental solutions in the form required by the BEM. In the case of elastic waves (Shaw and Manolis, 2000b) that are governed by vector differential equations, the class of solvable problems by this method is limited to variable (i.e., position dependent) density and constant elastic parameters. Even then, an additional assumption regarding decomposition of the displacement vector into pseudo-dilatational and pseudo-rotational parts is necessary in order to achieve a closed-form solution through reduction to the anti-plane strain case. The reason is that for a vector wave equation, the underlying coordinate transformation affects the base vectors of the gradient operator. Thus, the governing equations recovered in the transformed coordinate system are not necessarily simpler when compared to their original form. It is always possible, however, to construct a fine layer approximation for a heterogeneous medium, provided robust analytic solutions are available that remain stable at high frequencies of vibration (Tadeu and Antonio, 2001).

In order to overcome these difficulties, we employ Hormander's (1994) method, which uses matrix algebra formalism for the solution of systems of partial differential equations, as a more general approach for solving problems in elastic wave propagation through heterogeneous media under plane-strain conditions. An advantage of this method is that a key step in the solution procedure for these specific types of problems involves a biharmonic equation. If conditions of radial symmetry hold in the sense that material properties vary with respect to distance from the source of the disturbance (i.e., the origin of the coordinate system), then the biharmonic is a function of a single variable and becomes amenable to closed-form solution. Specifically, we focus on variable density profiles, but it is also possible to consider position-dependent elastic parameters (e.g., the Lamé constants). Furthermore, extension to $3D$ cases is rather straightforward. Briefly, the paper is structured as follows: Following development of the methodology for the $2D$ vector wave equation, some basic results are recovered for classical elastostatics and elastodynamics. Next, new results are derived for wave motion in medium with a variable density profile that approaches a constant (background) value at a distance comparable to a single wave length from the source of the disturbance. Finally, a numerical example serves to illustrate the present methodology and to highlight the differences observed in elastic waves as they propagate through a continuous medium that is no longer homogeneous.

2 Methodology

Consider a differential equation in the standard form

$$\mathbf{L}(\mathbf{u}) = \mathbf{f} \tag{1}$$

where $\boldsymbol{L}$ is the differential operator, $\boldsymbol{u}$ is the dependent variable and $\boldsymbol{f}$ is the forcing function, which from now on will be identified with the generalized Dirac delta function δ. At the same time, we will focus on the unbounded continuum (the elastic full-space), where the Sommerfeld radiation boundary condition is assumed to hold. Both $\boldsymbol{u}$ and δ are functions of the spatial variable $\boldsymbol{x}$ and, since time-harmonic conditions will be imposed, of the frequency parameter ω. Note that because of this last assumption, initial conditions are irrelevant. In terms of notation, we will interchangeably use bold symbols, index notation and brackets as a way of indicating vectorial quantities. It is obvious that any solution to eqn (1) as defined above can be viewed as a Green's function.

Following Hormander (1994) and using matrix notation, the solution for the dependent variable $\boldsymbol{u}$ can be written as

$$\{u\} = [L]^{-1}\{\delta\} = \frac{adj[L]\{\delta\}}{\det[L]} = adj[L]\{\phi\} \tag{2}$$

where *adj* and *det* respectively denote adjoint matrix and determinant. The intermediate scalar function ϕ is defined through the following equation:

$$\det[L(x)]\,\phi(x) = -\delta(x) \tag{3}$$

In mechanics, the delta function is viewed as a unit impulse to the system (here the continuous medium) at source point $\mathbf{x}$. If the impulse is applied in all three principal directions at $\mathbf{x}$, then a set of three displacement vectors results, which can be grouped column-wise to yield Green's tensor $\boldsymbol{G}$. Physically speaking, component G_{ij} is the displacement (although, depending on the definition of the dependent variable, it might be a force or any other type of reaction) at the receiver point in the i^{th}direction due to the aforementioned unit impulse placed at the source and in the j^{th}direction. The complete displacement solution u_i can therefore be synthesized in terms of Green's tensor as $\{u\} = [G]\{e\}$, where e_i is the unit base vector for the three principal directions.

Since we will restrict the present development to $2D$ (i.e., plane strain) conditions, eqn (1) corresponds to the following $2x2$ system of differential equations:

$$\begin{bmatrix} L_{11} & L_{12} \\ L_{21} & L_{22} \end{bmatrix} \begin{bmatrix} G_{11} & G_{12} \\ G_{21} & G_{22} \end{bmatrix} = \begin{bmatrix} 1 & 0 \\ 0 & 1 \end{bmatrix} (\delta) \tag{4}$$

where $\boldsymbol{L}$ has been decomposed into L_{ij} . Following eqs (2) and (3), the solution is

$$\begin{bmatrix} G_{11} & G_{12} \\ G_{21} & G_{22} \end{bmatrix} = \begin{bmatrix} L_{11} & -L_{12} \\ -L_{21} & L_{22} \end{bmatrix} (\phi) \tag{5}$$

where

$$(L_{11}L_{22} - L_{12}L_{21})(\varphi) = -\delta(\mathbf{x}) \tag{6}$$

In what follows, the above method will be validated against the 2D elastostatic operator.

2.1 Example: Elastostatics

The Green's function for 2D elastostatics using Hormander's method is evaluated here as a check. The governing equation of equilibrium in indicial notation is

$$(\lambda+\mu)\,u_{i,ij} + \mu u_{j,ii} + \delta(\mathbf{x})\,e_j = 0 \tag{7}$$

where u_i is the displacement vector, while the Lamé constants λ and μ are related through Poisson's ratio ν as $\lambda = \left\{2\nu/(1-2\nu)\right\}\mu$. Furthermore, commas indicate differentiation with respect to the spatial coordinates and the summation convention is implied for repeated indices that range as *i,j = 1,2*. Next, the G_{ij} tensor components are grouped as shown below

$$[L]\begin{Bmatrix} G_{11} \\ G_{21} \end{Bmatrix} = -\begin{Bmatrix} 1 \\ 0 \end{Bmatrix}\delta(\mathbf{x}) \text{ and } [L]\begin{Bmatrix} G_{12} \\ G_{22} \end{Bmatrix} = -\begin{Bmatrix} 0 \\ 1 \end{Bmatrix}\delta(\mathbf{x}) \tag{8}$$

and the differential operator $\boldsymbol{L}$ in eqn (7) is decomposed as follows:

$$L_{11} = \mu\nabla^2 + (\lambda+\mu)\frac{\partial^2}{\partial x^2}, L_{12} = L_{21} = (\lambda+\mu)\frac{\partial^2}{\partial x \partial y},$$
$$L_{22} = \mu\nabla^2 + (\lambda+\mu)\frac{\partial^2}{\partial y^2} \tag{9}$$

The intermediate step in eqn (6) requires solving the following biharmonic equation

$$\mu(\lambda+2\mu)\,\nabla^4\phi = -\delta(\mathbf{x}) \tag{10}$$

Under conditions of radial symmetry, the Laplacian is $\nabla^2 = \frac{1}{r}\left(\frac{d}{dr}\left(r\frac{d}{dr}\right)\right)$, so the biharmonic $\nabla^4\phi$ reads as

$$\nabla^4\phi = \frac{d^4\phi}{dr^4} + \frac{2}{r}\frac{d^3\phi}{dr^3} - \frac{1}{r^2}\frac{d^2\phi}{dr^2} + \frac{1}{r^3}\frac{d\phi}{dr} \tag{11}$$

The solution to the homogeneous part of eqn (10) is

$$\phi(r) = C_0 + C_1 r^2 + C_2 \ell n\left(r/r_0\right) + C_3 r^2 \ell n\left(r/r_0\right) \tag{12}$$

from which the last term also corresponds to the solution for a unit impulse at $r = 0$. The integration constant C_3 can be found by replacing this particular solution in eqn (10) and integrating both left and right hand sides around a disc centered at the origin whose radius in the limit tends to zero (Panc, 1975). The result (ignoring reference distance r_0) is

$$\phi(r) = -\frac{1}{8\pi}\frac{1}{\mu(\lambda+2\mu)}r^2\ell nr \tag{13}$$

Direct substitution of ϕ in eqn (5) yields

$$[G] = -\frac{1}{8\pi\mu(1-\nu)} \times \tag{14}$$
$$\begin{bmatrix} (3-4\nu)\ell nr - (x/r)^2 + C & -xy/r^2 \\ -xy/r^2 & (3-4\nu)\ell nr - (y/r)^2 + C \end{bmatrix}$$

which is identical to the solution recovered by Rizzo (1967) with the exception of the constant term *C=(3.5-4*ν) along the diagonal that signifies rigid body motion and can therefore be neglected. Finally, the two displacement components are reconstituted from the Green's tensor G_{ij} as $u_1 = G_{11}e_1 + G_{12}e_2andu_2 = G_{21}e_1 + G_{22}e_2$.

3 Governing equations of dynamic equilibrium

The governing equations for time harmonic elastodynamics in terms of the displacement vector (Navier's equations) are as follows (Achenbach, 1973):

$$(\lambda+2\mu)\,\nabla\nabla\cdot\mathbf{u} - \mu\nabla x\nabla x\mathbf{u} + \rho\omega^2\mathbf{u} = -\rho\mathbf{f} \tag{15}$$

This particular form requires constant elastic parameters λ and μ, but allows for a position-dependent density, namely $\rho(x,y)$. Also, **u** is the displacement vector and **f** is the body force vector per unit mass, taken here to be the unit impulse acting at source (x_0,y_0) and in both directions. Parenthetically, this implies that the reference value of density ρ is that registered at the source, since this is the only point where the body force is non-zero. Also, ω is the frequency at which the elastic wave propagates.

In solving the above equations for a variable density, the more standard forms obtained by the use of potentials are not useful, because of the need to differentiate Navier's equations at some point in order to form the two Helmholtz equations, whose fundamental solutions are easier to obtain (Manolis and Shaw, 2000). An alternative is to use dilatational and rotational displacement components, but again the two key vector operators in eqn (15) involving the gradient $(\nabla\,\bullet)$ and the curl $(\nabla\times)$ still have to be dealt with. Finally, conformal mapping techniques (Shaw and Manolis, 2000a) which hinge on producing simpler forms of eqn (15) in the new coordinate system also run into problems, because the base vectors underlying the gradient operator undergo a transformation in the new space and are responsible for the emergence of dispersive (i.e., velocity-dependent) terms that were originally absent.

For the homogeneous material case, fundamental solutions for eqn (15) under plane strain conditions can easily be found in the literature (Kobayashi, 1987). The basic structure of such a solution is $u_i = G_{ij} e_j$, with $i,j = 1,2$, where G_{ij} is given below as follows:

$$G_{ij} = \frac{i}{4\mu}\left\{G_1\delta_{ij} - G_2 \frac{\partial r}{\partial x_i}\frac{\partial r}{\partial x_j}\right\}$$

$$G_1 = H_0^{(1)}(k_s r) - \frac{1}{k_s r}H_1^{(1)}(k_s r) + \left(k_p^2/k_s^2\right)\frac{1}{k_p r}H_1^{(1)}(k_p r)$$

$$G_2 = -H_2^{(1)}(k_s r) + \left(k_p/k_s\right)^2 H_2^{(1)}(k_p r) \tag{16}$$

The above form is in terms of Hankel functions of the first kind, $H_n^{(1)}$,which represent outgoing waves. Also, the radial distance between receiver (x,y) and source (x_0,y_0) points is $r = \sqrt{(x-x_0)^2+(y-y_0)^2}$. The two wave numbers for pressure and shear waves are $k_p=\omega/c_p$ and $k_s=\omega/c_s$,respectively, while $c_p^2=(\lambda+2\mu)/\rho$ and $c_s^2=\mu/\rho$ are the corresponding wave velocities. An alternative form to that shown above can be obtained in terms of the modified Bessel functions K_0 for a complex argument (i.e., circular frequency ω is replaced by $i\omega$, $i=\sqrt{-1}$) based on the following relation:

$$K_0(kr) = \frac{\pi i}{2} H_0^{(1)}(ikr) \tag{17}$$

3.1 Example: Constant density elastodynamics

As before, in order to recover the elastodynamic Green's function using Hormander's method, we first write the Navier equations using indicial notation as

$$(\lambda+\mu)\,u_{i,ij} + \mu u_{j,ii} + \rho\omega^2 u_j = -\rho\delta(\mathbf{x})\,e_j \tag{18}$$

Then, Green's tensor G_{ij} is computed as follows:

$$[G_{ij}] = (1/\alpha)\begin{bmatrix} g_{11} & g_{12} \\ g_{21} & g_{22}\end{bmatrix} = [L]\phi =$$

$$\begin{bmatrix} \mu\nabla^2 + (\lambda+\mu)\frac{\partial^2}{\partial y^2} + \omega^2\rho & -(\lambda+\mu)\frac{\partial^2}{\partial x\partial y} \\ -(\lambda+\mu)\frac{\partial^2}{\partial x\partial y} & \mu\nabla^2 + (\lambda+\mu)\frac{\partial^2}{\partial x^2} + \omega^2\rho \end{bmatrix} \times$$

$$(\phi^p(r) + \phi^s(r)) \tag{19}$$

We note that α is a constant to be determined and that intermediate function ϕ is decomposed into a pressure wave component ϕ^p and a shear wave component ϕ^s. The determinant of the above $2x2$ matrix is computed as

$$\det[L(\mathbf{x})] = \mu(\lambda+2\mu)\nabla^4 + \rho\omega^2(\lambda+3\mu)\nabla^2 + \rho^2\omega^4 \tag{20}$$

Expanding the above determinant and rearranging terms yields a biharmonic equation

$$\nabla^4\phi + \left(k_p^2 + k_s^2\right)\nabla^2\phi + k_p^2 k_s^2\phi = -\frac{1}{\mu(\lambda+2\mu)}\rho\delta(r) \tag{21}$$

which can be factored into two Helmholtz-type equations as follows:

$$\left(\nabla^2+k_p^2\right)\left(\nabla^2+k_s^2\right)\phi(r)=-\frac{1}{\mu(\lambda+2\mu)}\rho\delta(r) \tag{22}$$

We seek solutions to the homogeneous form of eqn (22), so that each Helmholtz equation can independently go to zero. Furthermore, if radial symmetry can be invoked, then each of these two equations is a zero-order Bessel equation, i.e.,

$$\frac{d^2\phi(r)}{dr^2}+\frac{1}{r}\frac{d\phi(r)}{dr}+k^2\phi(r)=0 \tag{23}$$

where k corresponds to either k_s or k_p (and similarly ϕ is either ϕ^p or ϕ^s). The solution follows a scaling of r as kr (which brings about the standard form without any factor in front of $\phi(r)$) and is given below as

$$\phi(r)=AJ_0(kr)+BY_0(kr)=CH_0^{(1)}(kr)+DH_0^{(2)}(kr) \tag{24}$$

with J_0, Y_0 the Bessel functions and $H_0^{(1)}, H_0^{(2)}$ the Hankel functions, all of order zero. The latter are related to the former as

$$H_0^{(1,2)}(z)=J_0(z)\pm iY_0(z) \tag{25}$$

It is well known (Miklowitz, 1978) that the solution corresponding to outgoing waves generated by a unit impulse at the source can be recovered from the full homogeneous solution as $CH_0^{(1)}$,with C being an integration constant.

By substituting the Hankel function solution of zero order, first kind (with $C=1$) for $\phi(r)$ in eqn (19), we obtain the following results for the g_{ij}displacement tensor components:

$$g_{11}=\left(\rho\omega^2-k^2\mu\right)H_0^{(1)}(kr)+$$
$$(\lambda+\mu)\left\{-k^2H_0^{(1)}(kr)+\frac{k}{r}H_1^{(1)}(kr)-\frac{k^2x^2}{r^2}H_2^{(1)}(kr)\right\} \tag{26}$$

$$g_{22}=\left(\rho\omega^2-k^2\mu\right)H_0^{(1)}(kr)+$$
$$(\lambda+\mu)\left\{-k^2H_0^{(1)}(kr)+\frac{k}{r}H_1^{(1)}(kr)-\frac{k^2y^2}{r^2}H_2^{(1)}(kr)\right\} \tag{27}$$

and

$$g_{12}=-(\lambda+\mu)\frac{x}{r}\frac{y}{r}k^2H_2^{(1)}(kr) \tag{28}$$

We note here that the symbolic mathematics package Mathematica (1999), which was used in obtaining the above results, retains only the lowest order Bessel functions. In order to introduce $H_2^{(1)}$ so as to bring forth a form that can be compared with existing solutions, it is necessary to use the following Bessel function identity:

$$H_2^{(1)}(kr)=\frac{2}{kr}H_1^{(1)}(kr)+H_0^{(1)}(kr) \tag{29}$$

Synthesis of both pressure and shear wave components yields

$$\alpha G_{11}=g_{11}^P+g_{11}^S=$$
$$H_0^{(1)}(k_pr)\left\{\rho\omega^2-k_p^2\mu-k_p^2(\lambda+\mu)\right\}+$$
$$H_1^{(1)}(k_pr)\frac{k_p(\lambda+\mu)}{r}-H_2^{(1)}(k_pr)\frac{(\lambda+\mu)k_p^2x^2}{r^2}+$$
$$H_0^{(1)}(k_sr)\left\{\rho\omega^2-k_s^2\mu-k_s^2(\lambda+\mu)\right\}+$$
$$H_1^{(1)}(k_sr)\frac{k_s(\lambda+\mu)}{r}-H_2^{(1)}(k_sr)\frac{(\lambda+\mu)k_s^2x^2}{r^2}=$$
$$-k_s^2(\lambda+\mu)\left\{H_0^{(1)}(k_sr)+\frac{1}{k_sr}\left(H_1^{(1)}(k_sr)+\frac{k_p}{k_s}H_1^{(1)}(k_pr)\right)+\right.$$
$$\left.\frac{x^2}{r^2}\left(H_2^{(1)}(k_sr)+\frac{k_p^2}{k_s^2}H_2^{(1)}(k_pr)\right)\right\} \tag{30}$$

and

$$\alpha G_{12} = g_{12}^P + g_{12}^S \tag{31}$$

$$= -(\lambda+\mu)\frac{x}{r}\frac{y}{r}\left\{k_p^2 H_2^{(1)}(k_p r) + k_s^2 H_2^{(1)}(k_s r)\right\}$$

$$= -(\lambda+\mu)\,k_s^2\frac{x}{r}\frac{y}{r}\left\{H_2^{(1)}(k_s r) + \frac{c_s^2}{c_p^2}H_2^{(1)}(k_p r)\right\}$$

while the G_{22} component can be obtained from G_{11} by interchanging x and y. By comparing with the standard form of the solution as given by Kobayashi (1987) in eqn (16), constant α is determined as follows:

$$\frac{1}{\alpha} = \frac{i}{4\mu}\frac{1}{(\lambda+\mu)\,k_s^2} \tag{32}$$

More specifically, the presence of α is a consequence of the fact that the solution to eqn (22) was recovered from the homogeneous one given in eqn (24). Thus, two points have to be checked with respect to the Green's function, namely that: (a) it contains the correct singularity at the point of application of the point impulse (i.e., the origin), and (b) has the appropriate magnitude. The second point is rather mute, since there is certain latitude in the definition of the magnitude of the external impulse. For instance, Green's functions for Helmholtz's equation may correspond to factors of 4π, of 2π, or of unity in the right-hand side (Morse and Feshbach, 1953). Furthermore, it does not change the formulation of a BIEM statement (Cruse and Rizzo, 1968), since this involves the convolution of two distinct elastodynamic states, namely one corresponding to the actual boundary-value problem whose solution is sought, plus another involving the Green's function solution: obviously, the actual "strength" of this second state is unimportant.

3.1 The Green's function singularity

The singularity exhibited by Green's function around a disc of exclusion S_ε centered at the point of application of the impulse is now examined. Specifically, $\varphi(r)$ is assumed regular in the outer region S, while its singular part $\varphi^{si}(r)$ is computed by substituting back in the $2D$ Helmholtz equation (see eqn (23), but with $-\delta(r)$ as the right-hand side), integrating both sides around a disc of radius $r = \varepsilon$ centered at the origin and finally taking the limit as $\varepsilon \to 0$ (Morse and Feshbach, 1953). Since the singularity of the Laplacian of $\varphi^{si}(r)$ is obviously higher than the singularity of $\varphi^{si}(r)$ itself, the second term in the left-hand side of Helmholtz's equation is ignored. We therefore have that

$$\iint \nabla^2\varphi^{si}(r)\,dS_\varepsilon + 0 = -\iint \delta(r-0)\,dS_\varepsilon \tag{33}$$

The integral of the delta function is simply equal to 1.0, since disc S_ε includes the point of application of the impulse. For the other integral, we use Gauss' divergence theorem to get

$$\oint \nabla\bullet\varphi^{si}(r)\,d\Gamma_\varepsilon = -1 \tag{34}$$

where Γ_ε is the disc's perimeter. Given that $\varphi^{si}(r)$ is a function of the radius and that the gradient is normal to the disc's perimeter, the above integral is simply equal to

$$\left(\partial\varphi^{si}(r)/\partial r\right) = -1 \tag{35}$$

Thus, integration gives $\varphi^{si}(r) = -(1/2\pi)\ln(r)$ for $r \leq \varepsilon$, which is identical to the singular term in the Hankel function expansions for small argument.

4 Variable density elastodynamics

For this case we express the density, which is assumed to be dependent on the radial distance, in terms of a constant (or background) value denoted by subscript 0 plus a non-dimensional function $b(r)$ as

$$\rho(r) = \rho_0 b(r) \tag{36}$$

Similarly, $k(r) = k_0\sqrt{b(r)}$ is the expression for the generic wave number understood to represent both P and S waves.

Hormander's method, as previously developed, is applicable here as well. Specifically, the determinant of system matrix $L(\boldsymbol{u})$ acting on intermediate function $\phi(\boldsymbol{x})$ yields the following equation:

$$\mu(\lambda+2\mu)\nabla^4\varphi + (\lambda+3\mu)\,\omega^2\rho\nabla^2\varphi + (\lambda+3\mu)\,\omega^2\nabla\rho\cdot\nabla\varphi +$$
$$+\left(\rho^2\omega^2 + \frac{1}{2}(\lambda+3\mu)\,\omega^2\nabla^2\rho\right)\varphi = -\delta(x) \tag{37}$$

By comparing with the standard form given in eqn (20), we note the presence of two additional terms, namely one involving the gradient of the density (i.e., $\nabla\rho$) and another involving its Laplacian (i.e., $\nabla^2\rho$). At this stage, the solution will proceed ignoring these terms and their relative importance will be gauged once the corresponding density profile is recovered. Thus, it is still possible to factor the biharmonic equation for the variable density case into two Helmhotz equations, which however are no longer zero-order Bessel equations. Instead, they become Bessel equations of arbitrary order *n*, where *n* is not necessarily an integer. The reason is that we now have a variable wave number in eqn (23). Therefore, eqn (23) assumes the more general form given in Gradshteyn and Ryzhik (1980), which is given below as

$$\frac{1}{z}\frac{d}{dz}\left(zu'\right)+\left[\left(\beta\gamma z^{\gamma-1}\right)^2-\left(\frac{n\gamma}{z}\right)^2\right]u=0 \tag{38}$$

In the above, u and z are the dependent and independent variables, respectively, while β and γ are constants. The solution to eqn (38) is

$$u=\mathrm{Z}_n\left(\beta z^{\gamma}\right) \tag{39}$$

where Z_n stands for any of the Bessel functions J_n, Y_n or the Hankel functions $H_n^{(1)}, H_n^{(2)}$. Going back to the biharmonic equation, the obvious choice for $\phi(r)$ to represent outgoing waves is

$$\phi\left(r\right)=CH_n^{(1)}\left(kr^{\gamma}\right) \tag{40}$$

where $C$is the usual integration constant. As such, this new solution is a more general version of the basic solution used for constant density and reduces to it if $n=0$ and $\gamma=1$. By comparing eqs (23) and (38), the new wave number profile is

$$k^2=k_0^2\left\{\left(\gamma\, r^{\gamma-1}\right)^2-\frac{n^2\gamma^2}{k_0^2r^2}\right\} \tag{41}$$

For simplicity, we adopt $\gamma=1$ and thus $\phi=H_n^{(1)}(kr)$, while the corresponding two material profiles now simplify as

$$\rho=\rho_0\left(1-\frac{n^2}{k_0^2r^2}\right) \text{ and } k=k_0\sqrt{1-\left(\frac{n}{k_0r}\right)^2} \tag{42}$$

In reference to eqn (37), it is easy to show that $\rho(\boldsymbol{x})$ is an analytic function, which implies that $\nabla^2\rho(\boldsymbol{x})=0$. Furthermore, the density gradient with respect to radial distance r is equal to $\nabla_r\rho(r)=-2(n^2/k_0^2r^3)e_r$. Despite the fact that this gradient is not equal to zero, it is a rapidly decreasing function of r, especially in the region where the density profile approaches the constant value of ρ_0. Therefore, for all practical purposes, the gradient term does not influence the solution for the Green's function in the region where the density profile is positive. In any case, this term indicates dispersion, which can always be accounted for through the use of complex-valued wave numbers. In sum, the solution obtained here is approximate, and valid everywhere except in a small disc (whose radius is less than 10% of the value of the dominant wave length) in which the density profile assumes physically unreasonable negative values.

As before, substitution of $\phi(r)$ in eqn (19) with a variable density yields the following results for the g_{ij}components:

$$g_{11}=\frac{1}{4}\left\{4\rho\omega^2H_n^{(1)}+\frac{\mu x^2+(\lambda+2\mu)\,y^2}{r^2}\times\right. \\ k_0^2\left(H_{n-2}^{(1)}-2H_n^{(1)}+H_{n+2}^{(1)}\right)+ \\ \left.+2\frac{(\lambda+2\mu)\,x^2+\mu y^2}{r^3}k_0\left(H_{n-1}^{(1)}-H_{n+1}^{(1)}\right)\right\} \tag{43}$$

$$g_{12}=-\frac{1}{4}\left\{\frac{xy}{r^3}\left(\lambda+\mu\right)k_0\left[2H_{n+1}^{(1)}-2H_{n-1}^{(1)}\right.\right. \\ \left.\left.+rk_0\left(H_{n-2}^{(1)}-2H_n^{(1)}+H_{n+2}^{(1)}\right)\right]\right\} \tag{44}$$

$$g_{22}=\frac{1}{4}\left\{4\rho\omega^2H_n^{(1)}+\frac{(\lambda+2\mu)\,x^2+\mu y^2}{r^2}\times\right. \\ \left\{k_0^2\left(H_{n-2}^{(1)}-2H_n^{(1)}+H_{n+2}^{(1)}\right)+\right. \\ \left.+2\frac{\mu x^2+(\lambda+2\mu)\,y^2}{r^3}k_0\left(H_{n-1}^{(1)}-H_{n+1}^{(1)}\right)\right\} \tag{45}$$

In sum, the Green's function tensor is synthesized as follows: First, the components corresponding to the shear wave are $g^s_{11}, g^s_{12}, g^s_{22}$ and are derived from the $H^{(1)}_n((k_0 = k_{s0})r)$ Hankel function. Next, the process is repeated for the pressure wave components g^p_{11}, g^p_{12}, g^p_{22} coming from the $H^{(1)}_m((k_0 = k_{p0})r)$ Hankel function, where index $m \neq n$, as will be explained in the next section. Finally, the two solutions are superimposed as $g_{ij} = g^p_{ij} + g^s_{ij}$ and factor α that accounts for integration constant C is introduced, so as to yield the final form of the G_{ij} tensor. A cursory look at the biharmonic (i.e., eqn (22)) indicates that α can no longer have the same value as that given in eqn (32), because density ρ in the right-hand side is not constant and it's value at the origin does not coincide with the background value of ρ_0. This last step will be carried out in the next section, where the density profile is examined in more detail. Finally, since the impulse that triggers wave motion derives from a force per unit volume, the resulting displacement field represented by G_{ij} is measured in units of length.

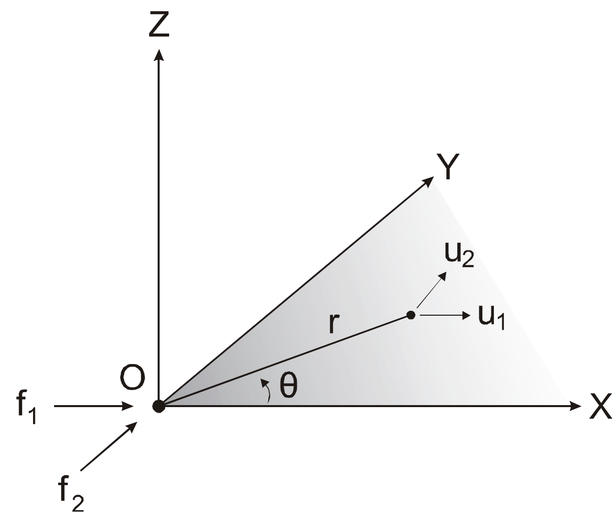

Figure 1 : Problem geometry with source at the origin and elastic wave polarization in the $x-y$ plane.

5 Numerical example

In order to investigate the effect of inhomogeneity derived from a position-dependent density on elastic waves propagating under time-harmonic conditions, we examine the case shown in Fig. 1 for a signal emanating from the origin outwards and restricted to travel on the $x-y$ plane. The geological medium in question (competent soft rock) is characterized by wave speeds c_p=*0.20 km/sec*,c_s=*0.10 km/sec* and by a Poisson's ratio ν=*0.33*. Also, the "background" density is ρ_0=*2,500 kg/m*^{3}. These values give the Lamé constants as λ=*5.0 10*^{9} and μ=*2.50 10*^{9} *kN/m*^{2}.Furthermore, we consider a low to intermediate frequency of transmission *f=2.0 Hz*, for which the following reference values for the pressure and shear wave numbers and their corresponding wave lengths are obtained:

$$\begin{aligned} k_{p_0} &= 6.28\,km^{-1}, \quad \lambda_{p_0} = 2\pi/k_p = 1.0\,km \\ k_{s_0} &= 12.57\,km^{-1}, \quad \lambda_{s_0} = 2\pi/k_s = 0.5\,km \end{aligned} \tag{46}$$

5.1 The Density Profile

The variable density profile is gauged with respect to the shear wave solution, i.e., $\rho(r)=\rho_0\{1-(n/k_{s0}r)^2\}$. Obviously, the value $n = 0$ corresponds to the homogeneous case, while for $n = 1$ we obtain a profile that is singular at the source (here the origin of the coordinate system) but rapidly approaches the background value ρ_0. Specifically, Fig. 2 plots these two cases, and for the latter one we observe that the density dips to negative values in an interval which is smaller than $r = 0.0795$ (i.e., for the first *7.95%* of the pressure wave length). At r=λ_{p0}, the material density has attained *99.4%* of the background value ρ_0. We mention in passing that the same profile is obtained for a negative value of the index, namely for $n = -1$. Finally, higher values of n yield density profiles which are less sharp than that previously mentioned. For instance, if $n = 2$, the density crosses to positive values at $r = 0.1591$ km from the source, while 97.4% of ρ_0 is obtained at r= λ_{p0}.

Since the density profile is unique for a given material, the following condition having to do with the presence of both pressure and shear waves in the continuum must hold true:

$$\rho(r) = \rho_0\left\{1-\left(n/k_{s0}r\right)^2\right\} = \rho_0\left\{1-\left(m/k_{s0}r\right)^2\right\} \tag{47}$$

From the above, $m/k_{p0} = n/k_{s0}$ and solving for the former index gives

$$m = \sqrt{(1-2\nu)\,/\,(2-2\nu)} \cdot n \tag{48}$$

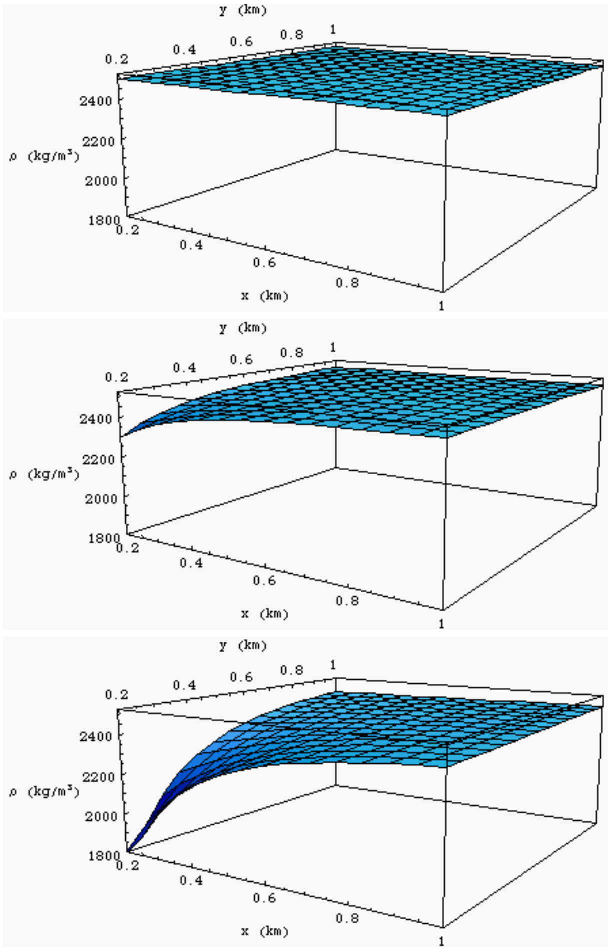

Figure 2 : Density ρ profiles as functions of index *n = 0, 1, 2* versus radial distance from the source.

Thus, for a Poisson's ratio of ν=*0.333*, $m = 1/2$ when $n = 1$. Other values of Poisson's ratio, such as ν=*0.25* and ν=*0.5*, respectively yield $m = 0.577$ and $m = 0$ with $n = 1$.

At this point, we wish to investigate the singularity exhibited by the density profile ρ*(r)* as a necessary step in computing factor α and thus complete the Green's function derivation given in section 4.As shown in Fig. 3, we take a disc of exclusion S_ε centered at the origin and define two points, **x** and ξ, which span the necessary distance r. The former is located on the perimeter of the disc, namely at distance ε from 0, while the latter is taken inside the disc at a distance $a < \varepsilon$, so as to avoid an unnecessary second singularity. Thus, we compute the limit as ε →*0* of the following integral:

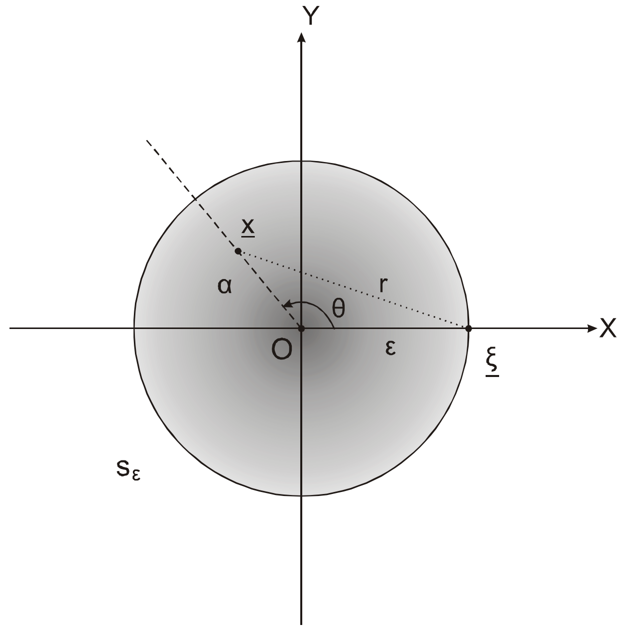

Figure 3 : Disc S_ε of infinitesimal radius ε around the singularity in the density ρ profile.

$$I_\varepsilon(x,\xi) = I_\varepsilon(r) = \iint cr^{-2}(x,\xi)\,dS_\varepsilon =$$

$$= c\int_0^{2\pi}\int_0^{\varepsilon}\frac{\varepsilon d\varepsilon}{r^2}d\theta = c\int_0^{2\pi} I_1(\varepsilon)d\theta \tag{49}$$

Constant $c = (n/k_{s0})^2$ is bounded and does not affect the integration. Carrying out the first integral with respect to ε (where the law of cosines is used to express r in terms of ε) yields

$$I_1(\varepsilon) = \int_0^{\varepsilon}\frac{\varepsilon d\varepsilon}{a^2+\varepsilon^2-2a\varepsilon\cos\theta} =$$

$$= \frac{1}{2}\ell n\left(a^2+\varepsilon^2-2a\varepsilon\cos\theta\right)\Big|_0^{\varepsilon} + \tag{50}$$

$$\frac{2a\cos\theta}{2}\left\{\frac{2}{2a\sin\theta}\arctan\left(\frac{2\varepsilon-2a\cos\theta}{2a\sin\theta}\right)\right\}\Big|_0^{\varepsilon}$$

Substituting the upper and lower limits of integration results in the following expression:

$$I_1(\varepsilon) = \ell n\sqrt{1+\left(\frac{\varepsilon}{a}\right)^2 - 2\left(\frac{\varepsilon}{a}\right)\cos\theta} +$$
$$\cot\theta \arctan\left[\frac{sin\theta}{(a/\varepsilon) - cons\theta}\right] \tag{51}$$

If we let b=ε/a, then we need to evaluate

$$I_\varepsilon = \lim_{b\to 0} c\int_0^{2\pi}\left\{\ell n\sqrt{1+b^2-2b\cos\theta}\right. \tag{52}$$
$$\left. + \cot\theta \arctan\frac{\sin\theta}{b-\cos\theta}\right\} d\theta$$

This last step is carried out using the Mathematica (1999) symbolic mathematics package, and results in $I_\varepsilon = -c\pi(\ell n4)$, where we note that the contribution of the logarithmic term in eqn (52) is actually zero. Thus, the singularity exhibited by the density at the point of application of the impulse function is a bounded one.

Factor α that was used in scaling the constant density Green's tensor in section 3 needs to be recomputed here. Specifically, the right-hand side of the biharmonic (eqn (22)) is now integrated over the disc of exclusion $S_\varepsilon$as follows:

$$-\iint \frac{1}{\mu(\lambda+2\mu)}\rho(r)\,\delta(r-0)\,dS_\varepsilon =$$
$$-\frac{1}{\mu(\lambda+2\mu)}\iint \rho_0\left\{1-\left(n/k_{s0}r\right)^2\right\}\delta(r)dS_\varepsilon \tag{53}$$

The first term in the above integral is the one that yielded the value of α given by eqn (32), while the second part furnishes a correction due to variability in the density profile. In order to compute this correction, we resort to the basic definition of the generalized delta function as a limiting process, since we are integrating over an infinitesimal disc centered at the origin whose radius ε is collapsing to zero. Specifically, the delta function is the limit of two Heaviside functions superimposed so as to produce a value of unity over the disc and zero elsewhere, as the disc radius goes to zero. Thus, the second part of the integrand in eqn (53) becomes

$$\frac{\rho_0}{\mu(\lambda+2\mu)}\left\{\left(n/k_{s0}\right)^2\iint\left(1/r\right)^2 dS_\varepsilon\right\} \tag{54}$$

and the expression inside the brackets is non other than I_ε that was previously evaluated. Thus, the corrected factor for variable density is simply $\alpha^{cor} = \alpha\{1.0+(n/k_{s0})^2\,\pi(\ell n4)\}$.

5.2 The Green's Function

In reference to eqs (43) to (45), the g^s_{ij} components are synthesized by using the $H_0^{(1)}$, $H_1^{(1)}$ and $H_2^{(1)}$ Hankel functions, while for the g^p_{ij}components we employ the fractional order Hankel functions $H^{(1)}_{(-1/2)}$, $H^{(1)}_{(1/2)}$ and $H^{(1)}_{(3/2)}$, as a consequence of eqn (48). In the latter case, the expansions used in computing of Bessel functions of fractional orders that are increments of an integer plus one-half are actually quite simple (Gradshteyn and Ryzhik, 1980). Specifically,

$$H^{(1)}_{(1/2)}(kr) = \sqrt{\frac{2}{\pi kr}}\frac{\exp(ikr)}{i} \tag{55}$$
$$H^{(1)}_{(-1/2)}(kr) = \sqrt{\frac{2}{\pi kr}}\exp(ikr)$$

and the standard recursion formula can be used for evaluating the necessary increments in order for the remaining Hankel functions. Finally, scaling the g_{ij} components by the corrected α^{cor} yields the final form of the Green's tensor G_{ij} for variable density elastodynamics in 2*D*.

5.3 Discussion of the Numerical Results

The Green's tensor components G_{11}, G_{12} and G_{22} are given in Figs. 4-6 for the homogeneous case $(n = 0)$ and in Figs. 7-9 for the variable density $(n = 1)$ case of eqn (47). In all cases, the graphs show both amplitude and phase angle for the particular displacement field that these tensor components represent. With respect to the former group of plots, we first observe the classical radiation decay in the amplitude, whereby the influence of the unit impulse at the origin decays rapidly by a factor of about ten as a distance equal to the pressure wave length is covered. Next, the phase angle plots are consistent with the fact that one cycle of vibration is anticipated across a distance of a single wave length.

As expected, variability in the density profile affects both the Green's function's amplitudes and phase angles. To that purpose, separate plots are provided in the form of Fig. 10 to help spot the differences, which are expressed as $\{(|G_{ij}^{heter}| - |G_{ij}^{homog}|)\ /\ |G_{ij}^{homog}|\ \}x\ 100$. We observe that in all cases, these fluctuations are more pronounced in the region close to the source, which is exactly where the density profile diverges the most from its background value. Both normal (G_{11}, G_{22}) as well as transverse $(G_{12} = G_{21})$ components exhibit the same amount of maximum fluctuation, which is roughly *20-25%*. The phase angle plots are also quite revealing, since the dip in the density profile seen in Fig. 2 influences the phase in the immediate vicinity of the source. In general, the variable density material examined herein, if the immediate neighborhood around the origin containing the unit impulse source is excluded, can probably be classified as weakly non-homogenous (Miklowicz, 1978), since it exhibits wave motion patterns that do not differ significantly from the ones expected in the case where the same material is homogeneous.

The final series of plots, Figs. 11-13, depict the usual Green's tensor components (G_{11}, G_{12} and G_{22}, respectively) for the variable density $(n = 1)$ case, but at a higher frequency of transmission *f=20.0 Hz*. In this case, both P and S wave numbers increase ten-fold compared to the values given by eqn (43), while their corresponding wave lengths are at one-tenth of their previous values. By observing these plots, we see (with difficulty) that they are not exactly scaled versions of the motions observed at the low frequency (*f=2.0 Hz*) end and given in Figs 7-9, because scaling factor α^{cor} is itself a function of frequency. Thus, the effect of a variable density profile of the type examined here is somewhat more noticeable at higher frequencies of vibration; this is in contrast to the standard homogeneous material, where obviously no such effect can be discerned.

In closing, we mention that the present Green's function is built on outgoing waves only, because of physical reasons. This implies that in more complex situations, where wave motions comprise both incoming and outgoing waves, plus the usual scattering phenomena associated with boundaries and interfaces, the effect of variable density will be more pronounced. The same comment holds true for higher-order Green's functions, such as F_{ij}, which corresponds to tractions at the receiver due to the same unit impulse at the source, since they derive from spatial integration of G_{ij}.

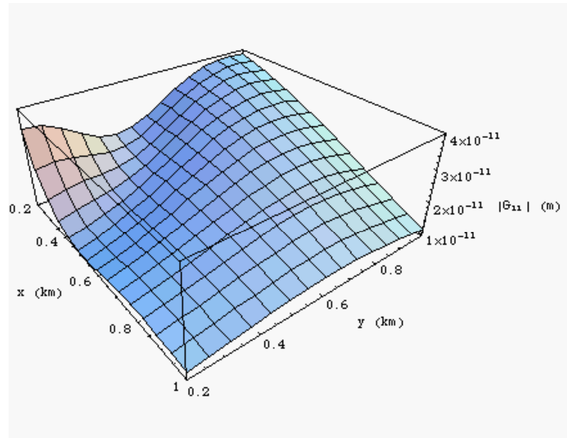

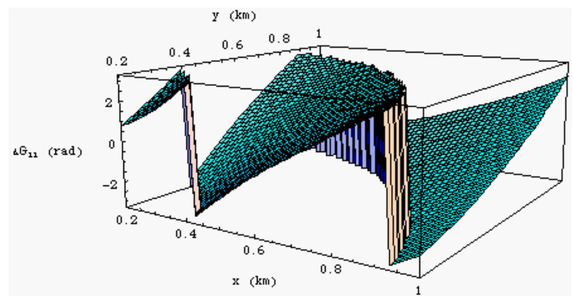

Figure 4 : Displacement component G_{11} vs. distance from source as function of index $n = 0$ and at frequency *f=2.0 Hz*: (a) amplitude and (b) phase angle.

5.4 General Comments on the Solution Procedure

There are some additional, and interesting from a mathematical viewpoint, comments with regards to the solution procedure used herein. Specifically, the final expression for the differential operator that results from an evaluation of the determinant of system matrix $\boldsymbol{L}(\boldsymbol{u})$ is dependent on the order by which the differentials are taken. This implies loss of symmetry, which can be explained using the following physical consideration: In a heterogeneous medium, the order of application of the point forces at the source influences the computation of the displacement signals at the receiver. To overcome this problem, we first apply forces of half magnitude using one order (x-direction first, y-direction second) and then the remaining magnitude using reverse order. This process is equivalent to a symmetrization of the differential operator given in eqn (1).

The solution for the differential operator given in eqn

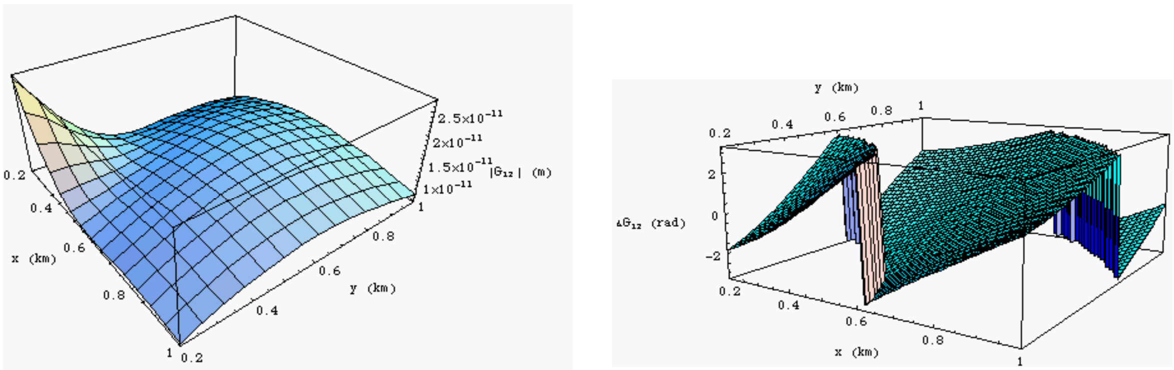

Figure 5 : Displacement component G_{12} vs. distance from source as function of index $n = 0$ and at frequency *f=2.0 Hz*: (a) amplitude and (b) phase angle.

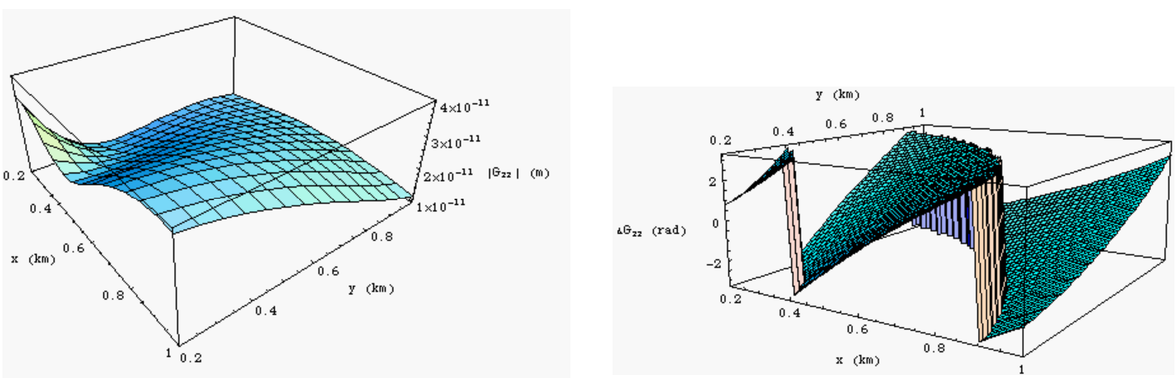

Figure 6 : Displacement component G_{22} vs. distance from source as function of index $n = 0$ and at frequency *f=2.0 Hz*: (a) amplitude and (b) phase angle.

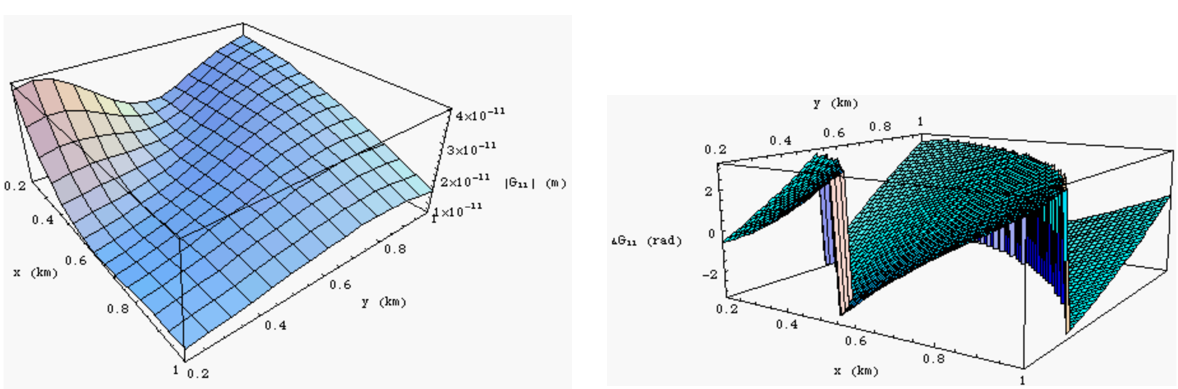

Figure 7 : Displacement component G_{11} vs. distance from source as function of index $n = 1$ and at frequency *f=2.0 Hz*: (a) amplitude and (b) phase angle.

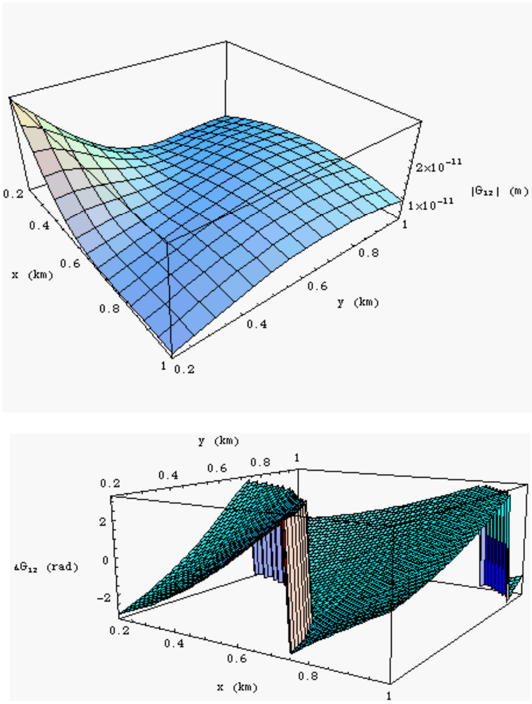

Figure 8 : Displacement component G_{12} vs. distance from source as function of index $n = 1$ and at frequency *f=2.0 Hz*: (a) amplitude and (b) phase angle.

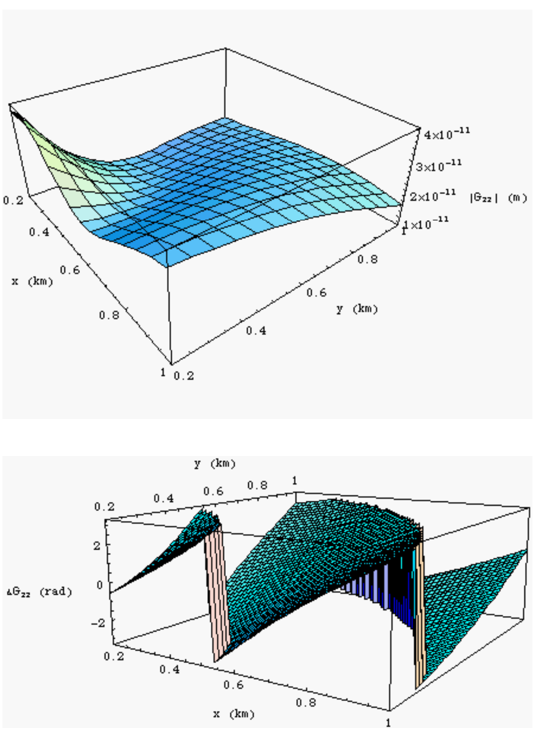

Figure 9 : Displacement component G_{22} vs. distance from source as function of index $n = 1$ and at frequency *f=2.0 Hz*: (a) amplitude and (b) phase angle.

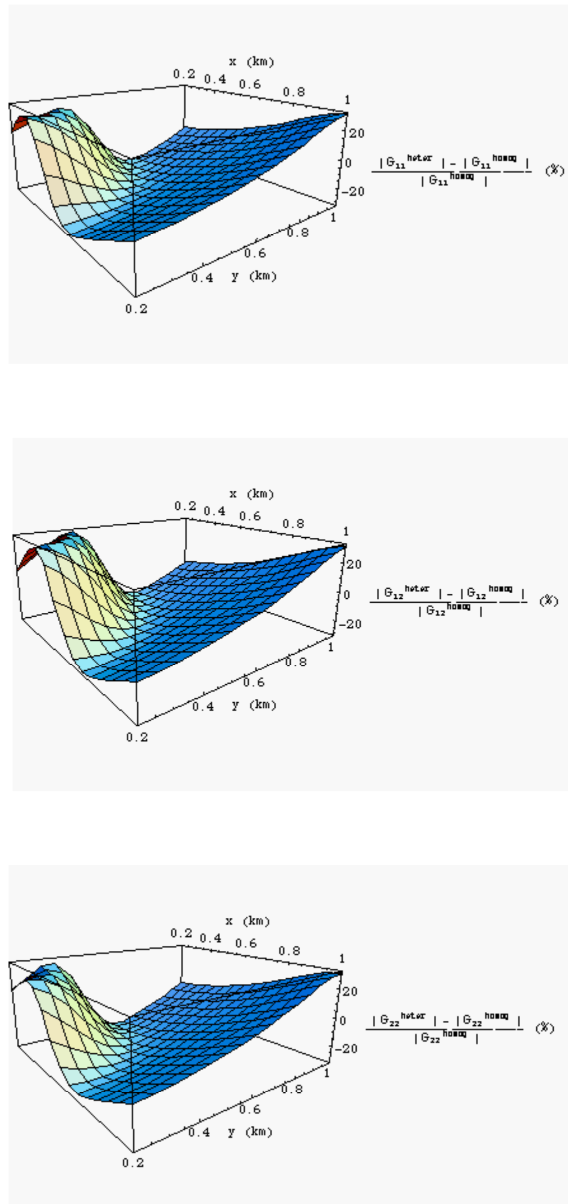

Figure 10 : Difference (as %) in the displacement component amplitudes (a) $G_{11,}$(b)G_{21} and (c) G_{22} for the heterogeneous case compared to the equivalent homogeneous material at a frequency *f=2.0 Hz*

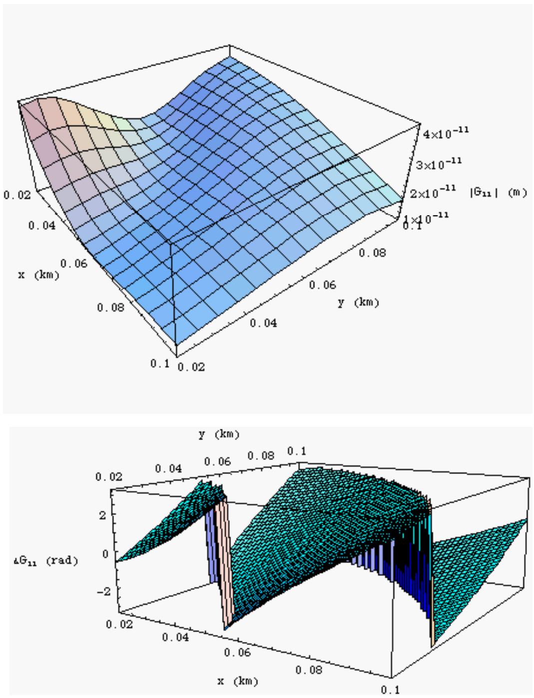

Figure 11 : Displacement component G_{11} vs. distance from source as function of index $n = 1$ and at frequency *f=20.0 Hz*: (a) amplitude and (b) phase angle.

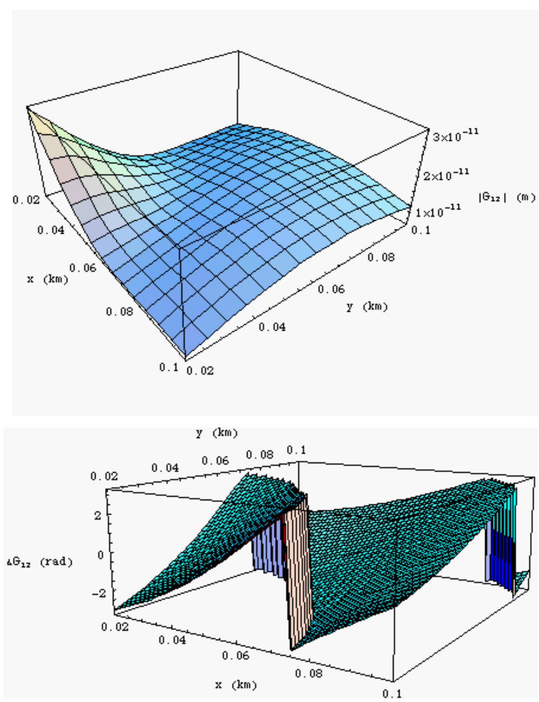

Figure 12 : Displacement component G_{12} vs. distance from source as function of index $n = 1$ and at frequency *f=20.0 Hz*: (a) amplitude and (b) phase angle.

(37) was obtained in what might seem a mathematically inconsistent way, despite the fact that it was checked afterwards. It turns out, however, that Hormander's method can be applied in a consistent way to variable density elastodynamics if the density term is convoluted with the dependent variable in the Navier-Cauchy equations, i.e.,

$$(\lambda + 2\mu)\,\nabla\nabla \cdot u - \mu\nabla \times \nabla \times u + \omega^2 \rho * u = -\rho * f \qquad (56)$$

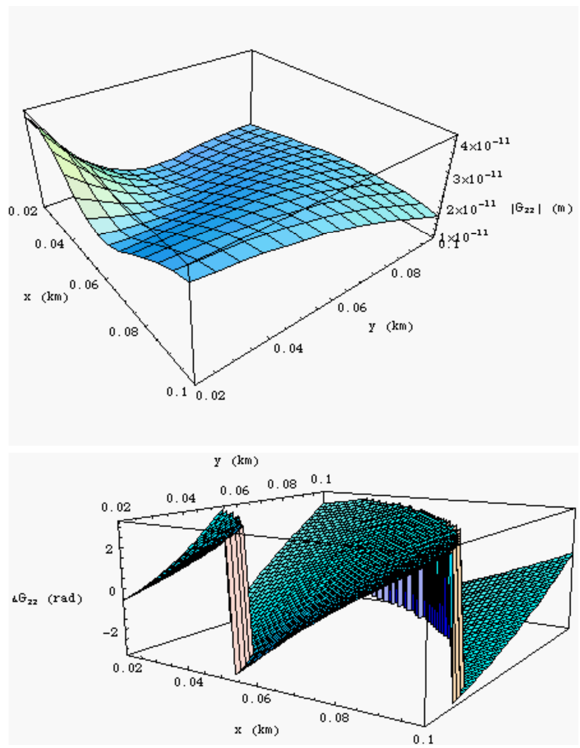

Figure 13 : Displacement component G_{22}vs. distance from source as function of index $n = 1$ and at frequency *f=20.0 Hz*: (a) amplitude and (b) phase angle.

where

$$\rho * u = \int \rho\,(r - s)\, u\,(s, \omega)\, ds \qquad (57)$$

This was recently examined in Rangelov and Manolis (2002) by using the double Fourier integral transformation with respect to the spatial variables, and a closed form transformed solution was obtained. It was then possible to show that the constant and variable density profiles such as those examined here can all be recovered as special cases from the general solution in the transformed domain. Of course, the inverse transformation for the general solution requires contour integration over the complex plane which is extremely difficult to do analytically, although in principle it is always possible to compute it numerically.

6 Conclusions

Although elastic wave propagation phenomena in inhomogeneous media are difficult to analyze, they have important applications to problems involving both manmade (e.g., composites) and naturally occurring (e.g., geological deposits) materials. In this work, we presented Hormander's method, which is based on matrix algebra formalism, for solving the governing partial differential equations of equilibrium in 2D elastodynamics. Subsequently, this method was applied to the variable density case, which is generally viewed as the simplest type of inhomogeneity. The methodology can, however, be extended to cover more general cases where all elastic constants become position-dependent. If these material parameters are functions of the radial distance from the source of the disturbance, then the underlying biharmonic equation is solvable in closed-form by a number of standard techniques. If, on the other hand, material parameter dependence is arbitrary in both planar directions, then the mathematical complexity increases substantially, because the biharmonic equation becomes a function of two independent variables. Finally, extension of the methodology presented herein to 3D problems is straightforward, since (a) the system matrix that yields the free-space Green's function is of size 3 (versus 2 before), and (b) if spherical symmetry applies to the variation of the material parameters, then the biharmonic equation remains a function of the radial distance and is, in principle, solvable.

7 References

Achenbach, J.D. (1973): *Wave Propagation in Elastic Solids*, North-Holland, Amsterdam.

Ang, W.T.; Kusuma, J.; Clements, D.L. (1996): A boundary element method for a second order, elliptic partial differential equation with variable coefficients, *Engineering Analysis with Boundary Elements*, 18, 311-316.

Bakirtas, I. (1984): The contact problem of an orthotropic non-homogeneous elastic halfspace, *International Journal of Solids and Structures*, 22(4), 347-351.

Beskos, D.E. (1987): Boundary element methods in dynamic analysis, *Applied Mechanics Reviews*, 40 (1), 1-23.

Beskos, D.E. (1997): Boundary element methods in dynamic analysis: Part II (1986-1996), *Applied Mechanics Reviews*, 50 (3), 149-197.

Clements, D.L. (1998): Fundamental solutions for second order linear elliptic partial differential equations, *Computational Mechanics*, 22, 26-31.

Cruse, T.A.; Rizzo, F.J. (1968): A direct formulation and numerical solution of the general transient elastodynamic problem: I, *Journal of Mathematical Analysis and Applications*, 22, 244-259.

Cruse, T.A. (1968): A direct formulation and numerical solution of the general transient elastodynamic problem: II, *Journal of Mathematical Analysis and Applications*, 22, 341-355.

Dominguez, J. (1993): *Boundary Elements in Dynamics*, Computational Mechanics Publications, Southampton.

Duffy, D.G. (1994): *Transform Methods for Solving Partial Differential Equations*, CRC Press, Boca Raton, Florida.

Ewing, W.M.; Jardetsky, W.S.; Press, F. (1957): *Elastic Waves in Layered Media*, McGraw-Hill, New York.

Geller, R.J.; Ohminato, T. (1994): Computation of synthetic seismograms and their partial derivatives for heterogeneous media with arbitrary natural boundary conditions using the direct solution method, *Geophysical International Journal*, 116, 421-446.

Gradshteyn, I.S.; Ryzhik, I.M. (1980): *Table of Integrals, Series and Products*, Academic Press, New York.

Gragg, R.F. (1998): One-way propagation in weakly nonuniform media, *Wave Motion*, 27, 95-115.

Gunturi, V.R.; Elgamal, A.W.M. (1998): A class of inhomogeneous shear models for seismic analysis of landfills, *Soil Dynamics and Earthquake Engineering*, 17, 197-209.

Guzina, B.B.; Pak, R.Y.S. (1996): Elastodynamic Green's functions for a smoothly heterogeneous halfspace, *International Journal of Solids and Structures*, 33(7), 1005-1021.

Hanyga, A. (1985): *Seismic Wave Propagation in the Earth*, Elsevier, Amsterdam.

Hazanov, S. (1999): On apparent properties of nonlinear heterogeneous bodies smaller than a representative volume, *Acta Mechanica*, 134, 123-134.

Helbig, K., (1994): *Modeling the Earth for Oil Exploration*, Pergamon/Elsevier, London.

Hormander, L. (1994): *An Analysis of Linear Partial Differential Operators, Vols. I-IV*, Springer-Verlag, Berlin.

Hryniewicz, Z.; Filipkowski, J. (1996): Dynamic stiffness matrix for in-plane motion in a layered, depth-dependent, randomly inhomogeneous semi-infinite medium, *Acta Mechanica*, 115, 39-54.

Itagaki, M. (2000): Advanced dual reciprocity method based on polynomial source and its application to eigenvalue problem for nonuniform media, *Engineering Analysis with Boundary Elements*, 24, 169-176.

Kobayashi, S. (1987): Elastodynamics, Chapter 4 in *Boundary Element Methods in Mechanics*, edited by D. E. Beskos, North-Holland, Amsterdam.

Manolis, G.D.; Beskos, D.E. (1988): *Boundary Element Methods in Elastodynamics*, Allen and Unwin, London.

Manolis, G.D.; Shaw, R.P. (2000): Fundamental solutions for variable density two-dimensional elastodynamic problems, *Engineering Analysis with Boundary Elements*, 24(10), 739-750.

Mathematica (1999): Version 4.0, Wolfram Research, Champaign, Illinois.

Melnikov, Y.A.; Melnikov, M.Y. (2001): Modified potentials as a tool for computing Green's functions in continuum mechanics, *CMES: Computer Modeling in Engineering and Sciences*, 2, 291-306.

Morse, P.M.; Feshbach, H. (1953): *Methods of Theoretical Physics, Parts I & II*, McGraw-Hill, New York.

Miklowitz, J. (1978): *Elastic Waves and Waveguides*, North-Holland, Amsterdam.

Muravskii, G. (2000): Parameter determination for a linearly inhomogeneous half-space using characteristics of the time harmonic surface waves, *Earthquake Engineering and Structural Dynamics*, 29, 399-418.

Muravskii, G.; Operstein, V. (1996): Time harmonic vibration of an incompressible linearly non-homogeneous half-space, *Earthquake Engineering and Structural Dynamics*, 25, 1195-1209.

Panc, V. (1975): *Theories of Elastic Plates*, Noordhoff Publishing, Leyden, Netherlands.

Rangelov, T.V.; Manolis G.D. (2002): On the existence of fundamental solutions for variable density elastodynamics, *Boundary Element Communications*, to appear.

Rizzo, F.J. (1967): An integral equation approach to boundary value problems of classical elastostatics, *Quarterly of Applied Mathematics*, 25, 83-95.

Selvadurai, A.P.S.; Lan, Q. (1998): Axisymmetric mixed boundary-value problems for an elastic half-space with periodic nonhomogeneity, *International Journal of Solids and Structures*, 35(15), 1813-1826.

Shaw, R.P.; Manolis, G.D. (2000a): A generalized Helmholtz equation fundamental solution using conformal mapping and dependent variable transformation, *Engineering Analysis with Boundary Elements*, 24(2), 177-188.

Shaw, R.P.; Manolis, G.D. (2000b): Elastic waves in one-dimensionally layered heterogeneous soil media, Chapter 6 in *Wave Motion in Earthquake Engineering*, edited by E. Kausel and G.D. Manolis, WIT Press, Southampton.

Tadeu, A.; Antonio, J. (2001): 2.5D Green's functions for elastodynamic problems in layered acoustic and elastic formations, *CMES:Computer Modeling in Engineering and Sciences*, 2, 477-496.

Vardoulakis, I.; Georgiadis, H.G. (1997) SH surface waves in a homogeneous gradient-elastic half-space with surface energy, *Journal of Elasticity*, 47, 147-165.

Volovoi, V.V.; Hodges, D.H.; Berdichevsky, V.L.; Sutyrin, V.G. (1998): Dynamic dispersion curves for non-homogeneous, anisotropic beams with cross-section of arbitrary geometry, *Journal of Sound and Vibration*, 215(5), 1101-1120.

Vrettos, C. (1998): The Boussinesq problem for soils with bounded non-homogeneity, *International Journal for Numerical and Analytical Methods in Geomechanics*, 22, 655-699.

Wang C.Y. (1998): Some exact solutions to the vibration of non-homogeneous membranes, *Journal of Sound and Vibration*, 210(4), 555-558.

Xu, S.Q.; Kamiya, N. (1998): A formulation and solution for boundary element analysis of inhomogeneous nonlinear problem, *Computational Mechanics*, 22, 367-37.